

# Development of Long-period Ground Motions from the Nankai Trough, Japan, Earthquakes: Observations and Computer Simulation of the 1944 Tonankai (Mw 8.1) and the 2004 SE Off-Kii Peninsula (Mw 7.4) Earthquakes

TAKASHI FURUMURA,<sup>1</sup> TOSHIHIKO HAYAKAWA,<sup>1</sup> MISAO NAKAMURA,<sup>2</sup> KAZUKI KOKETSU,<sup>1</sup> and TOSHITAKA BABA<sup>3</sup>

*Abstract*—Strong ground motions recorded in central Tokyo during the 1944 Tonankai Mw8.1 earthquake occurring in the Nankai Trough demonstrate significant developments of very large (>10 cm) and prolonged (>10 min) shaking of long-period ( $T > 10$ –12 s) ground motions in the basin of Tokyo located over 400 km from the epicenter. In order to understand the process by which such long-period ground motions developed in central Tokyo and to mitigate possible future disasters arising from large earthquakes in the Nankai Trough, we analyzed waveform data from a dense nation wide strong-motion network (K-NET and KiK-net) deployed across Japan for the recent SE Off-Kii Peninsula (Mw 7.4) earthquake of 5 September 2004 that occurred in the Nankai Trough. The observational data and a corresponding computer simulation for the earthquake clearly demonstrate that such long-period ground motion is primarily developed as the wave propagating along the Nankai Trough due to the amplification and directional guidance of long-period surface waves within a thick sedimentary layer overlaid upon the shallowly descending Philippine Sea Plate below the Japanese Island. Then the significant resonance of the seismic waves within the thick cover of sedimentary rocks of the Kanto Basin developed large and prolonged long-period motions in the center of Tokyo. The simulation results and observed seismograms are in good agreement in terms of the main features of the long-period ground motions. Accordingly, we consider that the simulation model is capable of predicting the long-period ground motions that are expected to occur during future Nankai Trough M 8 earthquakes.

**Key words:** Numerical simulation, finite-difference method, strong ground motion, long-period ground motion, Tonankai earthquake.

## 1. Introduction

Large M 8 earthquakes have occurred repeatedly in the Nankai Trough at a recurrence period of about 90–110 years. The 1944 Tonankai (Mw 8.1) earthquake

---

<sup>1</sup> Earthquake Research Institute, University of Tokyo, 1-1-1 Yayoi, Bunkyo-ku 113-0032, Japan.  
E-mail: furumura@eri.u-tokyo.ac.jp

<sup>2</sup> Information Service for Disaster Prevention, 230-7 Miroku-machi, Sakura, Chiba 285-003, Japan.

<sup>3</sup> IFREE, Japan Agency for Marine-Earth Science and Technology, 3172-25 Showa-machi, Kanazawa-ku, Yokohama, Kanagwa 236-0001, Japan.

resulted in more than 1250 deaths along the Pacific-facing southern coast of Japan. During this event, high seismic intensities ( $>5$  on the 7-point scale of the Japanese Meteorological Agency (JMA)) were recorded along the southern coast of central Japan, more than 100 km from the source region of the earthquake (USAMI, 1996).

Tokyo, the largest population center in Japan, is located about 400 km from the hypocenter, and recorded a maximum intensity of 3–4 on the JMA scale. No significant damage was reported in Tokyo during the large but distant earthquake; however, ground motions recorded in Tokyo demonstrate the development of very large ( $>10$  cm) and prolonged ( $>10$  min) shaking, dominated by long-period ( $T_0 = 10\text{--}13$  s) ground-shakings generated by the earthquake (FURUMURA and NAKAMURA, 2006).

Such strong and prolonged shaking of long-period ground motions within sedimentary basins brings to mind the extensive damage and fires in oil-storage tanks during the 2003 Tokachi-oki (Mw 8.0) earthquake (e.g., HATAYAMA *et al.*, 2004; KOKETSU *et al.*, 2005). The 2004 Chuetsu Niigata earthquake (Mw 6.6) significantly effected on tall buildings of approximately 70 floors, with a resonance of long-period ground motions of approximately 7 s recorded in central Tokyo (FURUMURA and HAYAKAWA, 2007). These observations warn of the potential vulnerability of modern large-scale construction to large earthquakes occurring around Tokyo. Thus, it is urgent to investigate the processes by which long-period ground motions within the Kanto Basin originate and evolve. This will aid in the mitigation of future seismic-related disasters predicted to result from earthquakes in the Nankai Trough.

The Mw 7.4 SE Off-Kii Peninsula earthquake occurred in the Nankai Trough, southwest of Kii Peninsula, Japan, at 23:57 JST on 5 September, 2004. Although the maximum intensity recorded in Tokyo was less than 2 on the JMA scale, most of the Tokyo area was subjected to more than 5 minutes of intense ( $>5$  cm) ground-shaking and a relatively long dominant period of about 7–12 s (e.g., HAYAKAWA *et al.*, 2005; MIYAKE and KOKETSU, 2005). These large and prolonged long-period ground motions led to significant resonance to large-scale oil-storage tanks in the area around Tokyo Bay and caused damage to the floating roofs of the tanks (HATAYAMA *et al.*, 2005), highlighting the risk to modern large-scale construction posed by large earthquakes.

Although the strong motions generated during the 1944 Tonankai earthquake were recorded on only a few distant stations such as installed in Tokyo (most of the near-field stations were clipped by the intense ground-shaking), ground motions associated with the 2004 SE Off-Kii Peninsula earthquake were clearly recorded by more than 500 stations of the high-density nation wide strong-motion network of K-NET and KiK-net across Japan. Thus, observations from the 2004 event provide us with a detailed understanding of the nature of long-period ground motions that affected central Tokyo during the earthquake in the Nankai Trough.

To complement the observational data and provide insight into the complexities of seismic behavior which result from interaction between complex 3D subsurface structure along the propagation path, we conducted large-scale computer simulations of seismic waves propagation during the 2004 SE Off-Kii Peninsula earthquake and the 1944 Tonankai earthquake. In conducting these simulations, we used the Earth Simulator

supercomputer with a high-resolution subsurface structure model of central Japan and an appropriate source-slip model for the earthquakes. Snapshots of seismic wave propagation during these events, as well as waveforms derived from the simulation and comparisons with observed seismograms provide for a detailed understanding of the nature of the seismic wavefield and the development of intense and prolonged long-period ground motions within central Tokyo.

## 2. Long-period Ground Motions Associated with the 2004 SE Off-Kii Peninsula Earthquake

Figure 1 shows snapshots of ground motions resulting from the SE Off-Kii Peninsula earthquake, as recorded by the K-NET and KiK-net strong-motion network using a

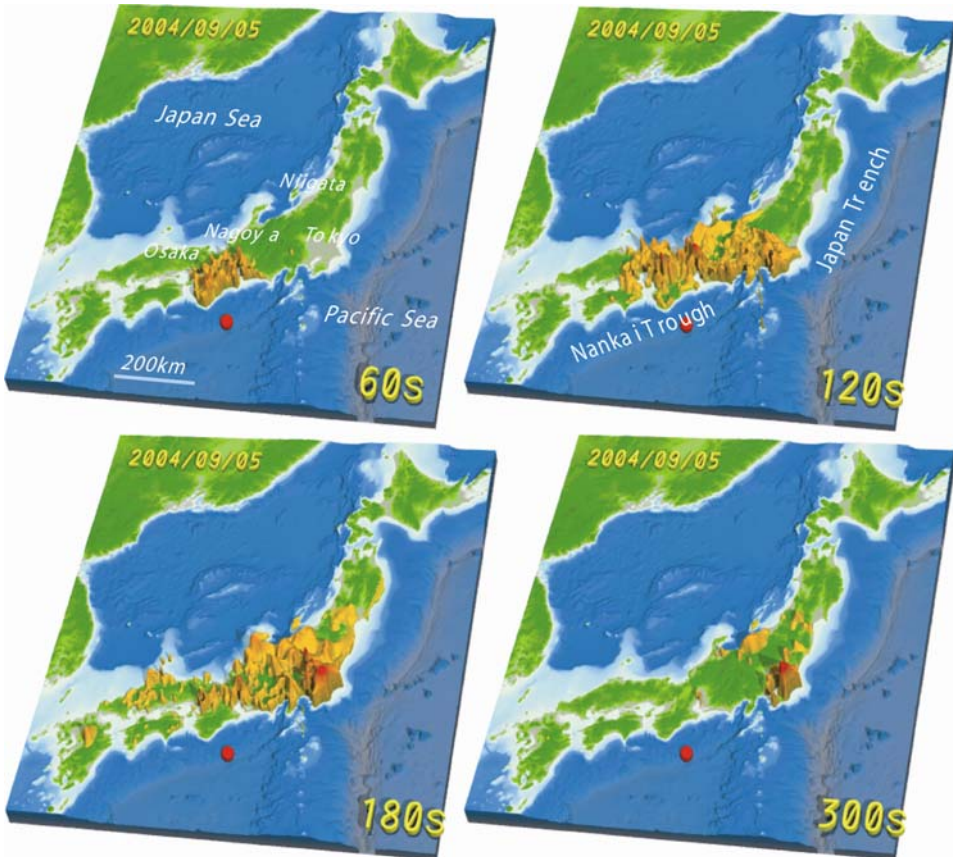


Figure 1

Snapshots of seismic wave propagation following the 2004 SE Off-Kii Peninsula earthquake, Japan. The hypocenter of the event is marked by a red circle. The distribution of horizontal velocity ground motions is shown for times of  $T = 60, 120, 180,$  and  $300$  s following the earthquake rupture.

visualization procedure for the seismic wavefield (FURUMURA *et al.*, 2003). Each snapshot shows the spatial and temporal distribution of ground motions at a given time from the earthquake rupture. The ground accelerations observed at 512 strong-motion stations are integrated into ground velocity motions in order to enhance the contribution of long-period ground motions with period of over 1 s. The amplitude of horizontal ground motion at each point is multiplied by the epicentral distance for roughly compensated geometrical attenuation and then logarithmically compressed in order to display a wide range of ground motions from source region to regional distances.

The first snapshot ( $T = 60$  s) shows intense ground-shaking in the area closest to the source region. A significant amplification of ground motions in sedimentary basins resulted in very strong and prolonged ground motions, which is apparent in large basins such as in Osaka and Nagoya in the 120 s snapshot and in Toyama and Niigata in the 180 s snapshot.

The attenuation of short-period surface waves is evident as the seismic waves spread from the source region, However the amplitude of the ground motion is reinforced significantly when entering the large Kanto Basin (Tokyo region). Ground motion in the Kanto Basin is at least 10-times greater than that measured in surrounding areas. The 300 s snapshot shows that intense and prolonged ground motions occurred in the Kanto Basin for more than several minutes, clearly outlining the basin margins.

Figure 2 shows the distribution of ground motions associated with the earthquake in terms of seismic intensity, peak ground acceleration (PGA), and peak ground displacement (PGD). The attenuation properties of the short-period ground motions (with periods of less than about 1 s) are well illustrated by PGA (Fig. 2b) and seismic intensity (Fig. 2a). Both PGA and seismic intensity show subcircular distributions above the hypocentral area, with pockets of greater amplification in the Nagoya and Osaka Basins resulting from the amplification of short-period ground motions within shallow covering layers in the sedimentary basins.

The attenuation of short-period seismic waves in the Kanto area is significant, and the maximum intensity is less than 2; however, the PGD map shows surprisingly enhanced ground motions in the Kanto Basin, in excess of 5 cm (Fig. 2c). Large PGD is also recorded in other major sedimentary basins such as those in Osaka, Nagoya, Toyama, and Niigata, although the anomalously large PGD of more than 5 cm recorded for Tokyo is very surprising, given the distance from the hypocenter ( $>400$  km) and the intermediate magnitude ( $M_w$  7.4) of the event.

As is evident in the waveforms of ground displacement motion recorded at K-NET stations (OSK005, AIC003, TYM005, YMN005, and TKY025; see Fig. 2c) located upon major basins, the large PGD recorded in major population centers and in Tokyo is caused by large, long-period surface waves that developed within thick sedimentary basins (Fig. 2d).

Figure 3 shows the velocity response spectra of horizontal ground motion recorded in each station and assumed a damping coefficient of  $h = 0.05$ . As the K-NET and KiK-net recordings rely on an event-trigger system, weak initial P and S waves and later coda with relatively small acceleration levels were not recorded by the strong motion instruments.

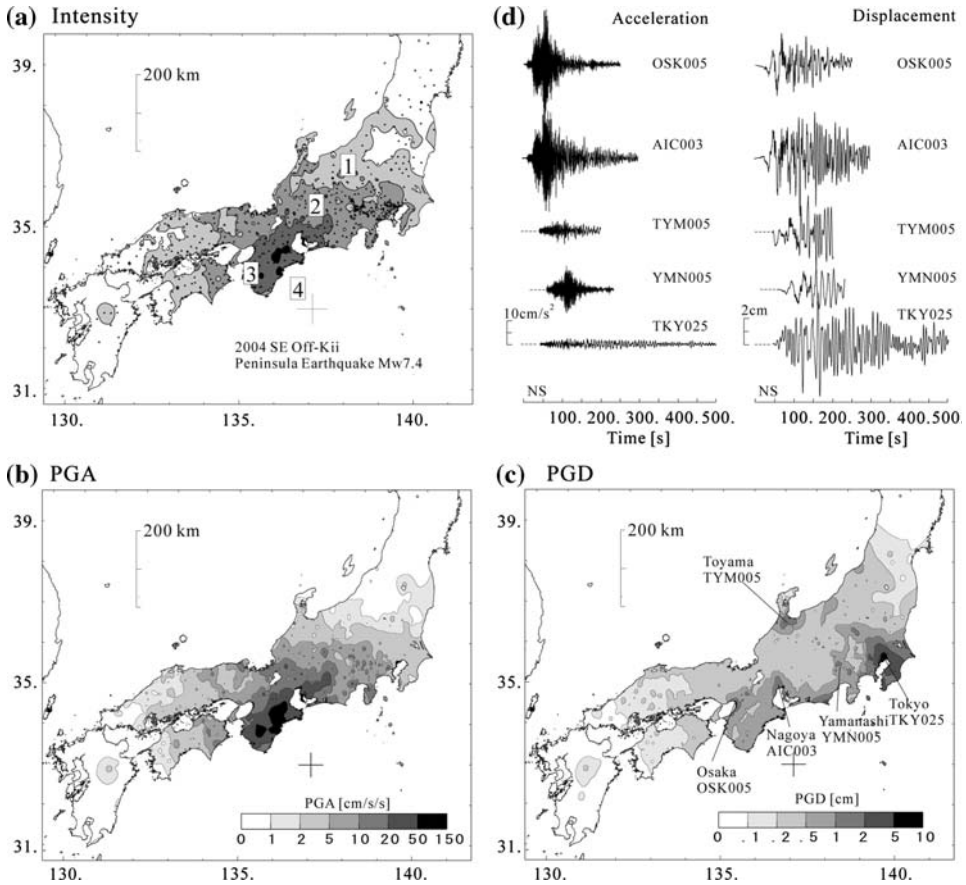


Figure 2

Distribution of (a) seismic intensity in terms of the JMA 7-point scale (small triangles denote K-NET and KiK-net stations that were triggered during the earthquake), (b) peak ground acceleration (cm/s/s), and (c) peak ground displacement (cm) during the 2004 SE Off-Kii Peninsula earthquake. (d) Wave form of NS-component ground acceleration and displacement recorded at five K-NET stations (OSK005, AIC003, TYM005, YMN005, and TKY025).

However, even in the short-duration recordings, significant resonance of the long-period ground motions in sedimentary basins is clearly displayed with a sharp peak in resonance periods of about 2 s for Nagoya (AIC003), about 3 s for Osaka (OSK005), and about 6 s for Toyama (TYM005). The very large response of over 10 cm/s in central Tokyo (TKY024) is almost as large as that observed near the source region.

MIYAKE and KOKETSU (2005) studied the spatial distribution of the dominant period of long-period ground motions generated during the 2004 SE Off-Kii Peninsula earthquake by employing high-density records of intensity meters located at e.g., the city government office and fire stations, as well as using K-NET and KiK-net data. The detailed map arising from their study demonstrates that long-period ground motions with a dominant

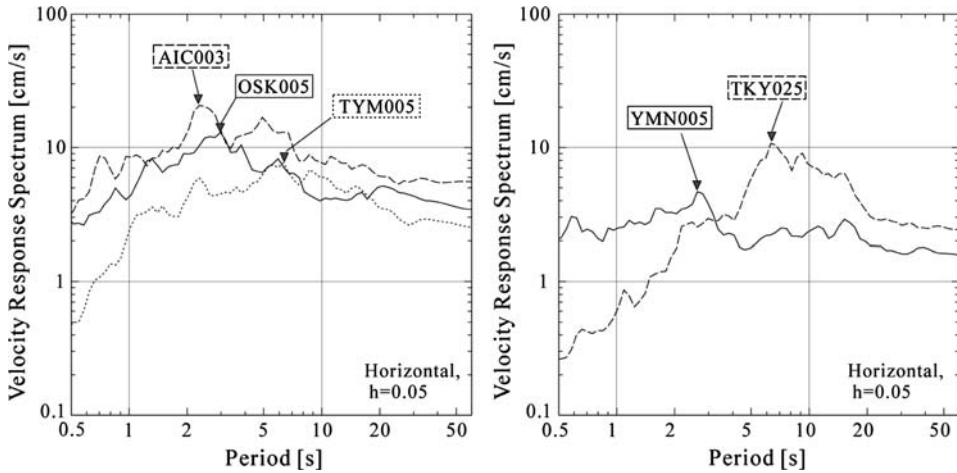


Figure 3

Velocity response spectra of observed ground motions recorded at stations AIC003, OSK005, TYM005, YMN005, and TKY025, assuming a damping coefficient of  $h = 0.05$ . The first peak of each resonance period is marked by a triangle.

period of around 7–12 s developed in the Tokyo Bay area during the earthquake. These results are consistent with reports that oil-storage tanks experienced a resonance period of about 6–12 s, resulting in sloshing of the oil and damage to the tanks during the earthquake (HATAYAMA *et al.*, 2004).

To study the progressive development of such long-period ground motions from the source area in the Nankai Trough toward the Kanto Basin more thoroughly, we compiled the observed waveforms of seven linearly aligned K-NET stations from the Kii Peninsula to central Tokyo (Fig. 4, line a–a').

Close to the source region, short-period (<1 s) S waves are the main contributor to horizontal ground motions, but attenuation of the short-period signals becomes severe with increasing distance from the hypocenter. In contrast, long-period ground motions with a dominant period of about 7–10 s that follows the S waves gradually acquire a greater amplitude with propagation along the coast, and these waves are the principle contributor to the observed large and prolonged ground motions, as depicted in the snapshots (Fig. 1) and PGD map (Fig. 2c). The group velocity of the, long-period, later signals is less than about 1 km/s, thus, we can recognize the long-period signals as surface waves which developed near the hypocentral area by the conversion of S waves radiating from the shallow ( $h = 8$  km) earthquake source. As these later signals are clearly depicted in transverse and radial motions, we are able to recognize that the mixing of Rayleigh and Love waves is the major component of the surface wave.

A number of recent reflection and refraction experiments in the Nankai Trough (e.g., TAKAHASHI *et al.*, 2002; NAKANISHI *et al.*, 2002; KODAIRA *et al.*, 2005) have demonstrated a thick cover of oceanic sediments (>5–10 km) above the shallowly subducting Philippine Sea Plate, forming a low-wavespeed accretionary prism above the subduction zone. This

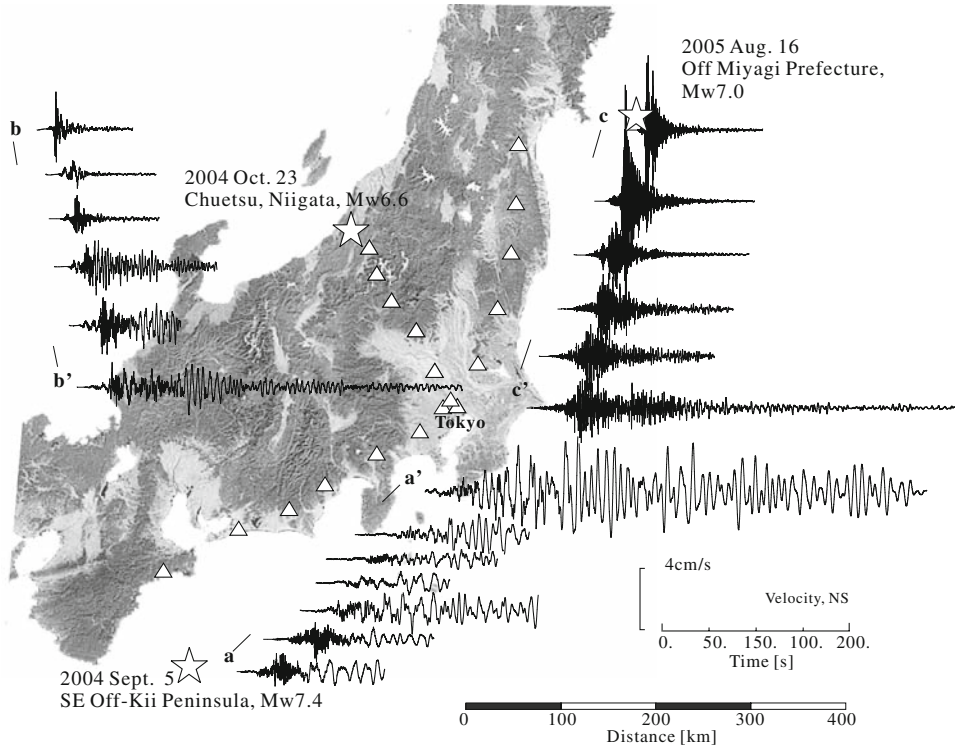


Figure 4

Recorded sections of NS-component ground velocity motions associated with the 2004 SE Off-Kii Peninsula earthquake (a–a'), the 2004 Chuetsu, Niigata earthquake (b–b'), and the 2005 Off Miyagi Prefecture earthquake (c–c'), illustrating the development of long-period surface waves during propagation of the waves from the source region to central Tokyo.

thick cover of sediments upon the subducting plate, and the large velocity contrast across the sediment–plate interface, are considered to contribute strongly to the efficient development of large surface waves and the guiding of seismic waves toward Tokyo. The importance of the low-wavespeed accretionary prism covering the subducting plate on the developments of long-period surface waves has been noted by SHAPIRO *et al.* (2000) as an important mechanism of the development of prolonged ground motions observed in Mexico City during large subduction zone earthquakes.

As the seismic wave that propagates to the Kanto Basin along the Nankai Trough already has a large and very lengthy wavetrain, and as entering the thick cover of sediments below the Kanto Basin it changes to another type of surface wave, induced by conversion and a scattering of incidental waves at the edge of the basin. Consequently, the resulting surface waves within central Tokyo are at least several times larger and longer than the original motions outside the basin.

We compared the development of long-period surface waves in the Kanto Basin that originated from large recent earthquakes located near Tokyo: a shallow ( $h = 15$  km)

inland Mw 6.6 earthquake at Chuetsu, Niigata on October 23, 2004 (Fig. 4, line b–b'), and a relatively deep ( $h = 42$  km) Mw 7.0 subduction zone earthquake off Miyagi Prefecture on 16 August, 2006 (Fig. 4, line c–c').

A plot of the progression of seismic waves from the Chuetsu earthquake to central Tokyo clearly demonstrates the development of surface waves in the Kanto Basin induced by conversion from S waves at the northern edge of the Kanto Basin (Fig. 4, line b–b'). The amplitude and duration of the surface waves gradually increased as they approached central Tokyo, but the developing properties and the duration of the surface waves was very mild compared to those of the 2004 SE Off-Kii Peninsula earthquake. The Off Miyagi Prefecture earthquake, a relatively deep ( $h = 42$  km) event that occurred upon the subducting Pacific Plate in the Japan Trench, produced a very weak surface wave following a large, short-period S wave with long coda. It is widely recognized that deep earthquakes upon the subducting Pacific Plate show anomalously large ground acceleration and intensity along the eastern seaboard of the Pacific Ocean due to the guiding of short-period ( $T < 0.5$  Hz) signals along the subducting plate. This occurs because of the multiple forward scattering of short-period signals within small-scale heterogeneities inside the plate (e.g., FURUMURA and KENNETT, 2005), but long-period signals with longer wavelengths do not capture such small-scale heterogeneities.

Consequently, of the three earthquakes that have recently occurred around Tokyo, shallow earthquakes in the Nankai Trough are potentially the most disastrous in terms of generating strong, prolonged long-period surface waves in the direction of central Tokyo. Thus, we anticipate a significant impact in Tokyo associated with M8 earthquakes in the Nankai Trough.

### *3. Long-period Ground Motions Arising from the 1944 Tonankai Mw 8.1 Earthquake*

Long-period ground motions that occurred in Tokyo during the Mw 8.1 Tonankai earthquake in 1944 were well documented by the Imamura-type strong-motion instruments (natural period of 3–5 s and magnification of 2) and the Central Meteorological Observatory (CMO)-type strong-motion instruments (natural period of 3–5 s and a magnification of 1) installed in the seismic observatory in central Tokyo (Otemachi), at Chiba (Togane), and at Yokohama (Fig. 5).

The JMA has compiled historical strong-motion seismograms for major damaging earthquakes since 1927, and the data are available on a microfilm database. The Earthquake Research Institute of the University of Tokyo also has an archive of historical recordings of strong-motion instruments since 1920. We obtained recordings of strong motions in Tokyo during the 1944 Tonankai earthquake (FURUMURA and NAKAMURA, 2006), and will make use of these data in studying the characteristics of long-period ground motions in Tokyo arising from large M 8 earthquakes in the Nankai Trough.

In contrast to the ease of analysis of modern, high-quality digital seismograms, the smoked-paper seismograms of early strong-motion instruments is rather perplexing;



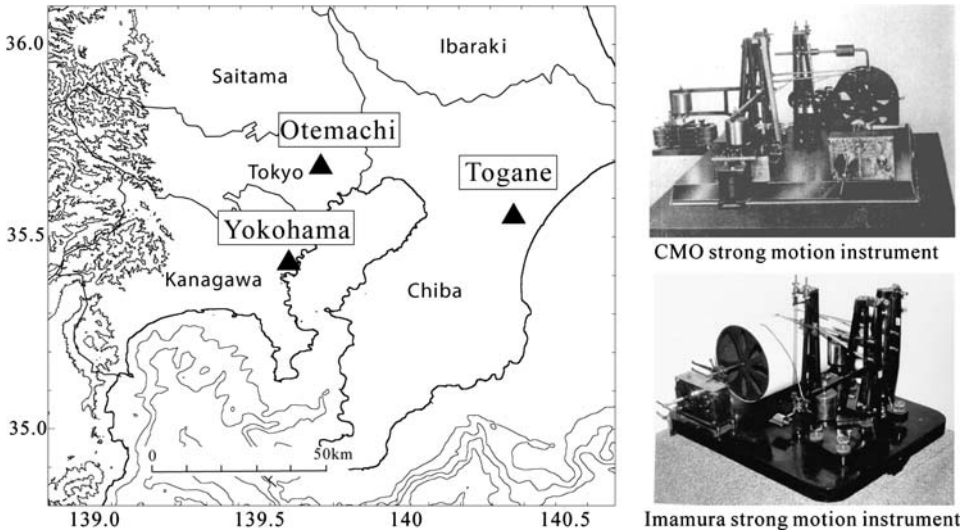


Figure 5

Map showing the locations of strong-motion stations that recorded strong ground motions during the 1944 Tonankai earthquake. The photographs show the CMO-type strong-motion instrument that was installed at Otemachi (upper) and the Imamura-type strong-motion instrument that was installed at Togane and Yokohama (lower).

however, recent developments of functional image-processing software made it possible to analyze these historical records (Fig. 6). The continuous recording method employed by these seismometers captured the entire record of the strong ground motions that occurred in Tokyo during the Tonankai earthquakes.

Images of the original smoke-paper seismograms were first captured using a scanner at high resolution (600 dpi) and are then digitized by hand tracing at small time intervals of less than 0.1 s. The digitized data set was corrected for pen-arc and base-line errors, and the digital waveform was then resampled with a uniform sampling interval of 10 Hz. Due to the effect of pen friction in the early seismometers, the effective frequency range of the seismogram is below about 1 Hz, so that we applied a bandpass filter to the waveform data with a bandpass frequency between 0.02 and 1 Hz.

Finally, the reproduced waveforms of the horizontal motions of the strong-motion instruments were translated to actual ground motions by removing the instrumental response from the recorded waveforms. Instrumental constants such as the natural period ( $T_0$ ) and the damping constants ( $h$ ) were obtained for each component of the seismometers by analyzing the time history of the impulse response curve recorded on the same seismograph paper.

We finally obtained the strong ground motions of horizontal ground displacement during the 1944 Tonankai earthquake at Togane, Otemachi, and Yokohama (Fig. 7). The reproduced ground motions resulting from the Tonankai earthquake, which were at least 2.5 times larger and several times longer than those recorded during the SE Off-Kii

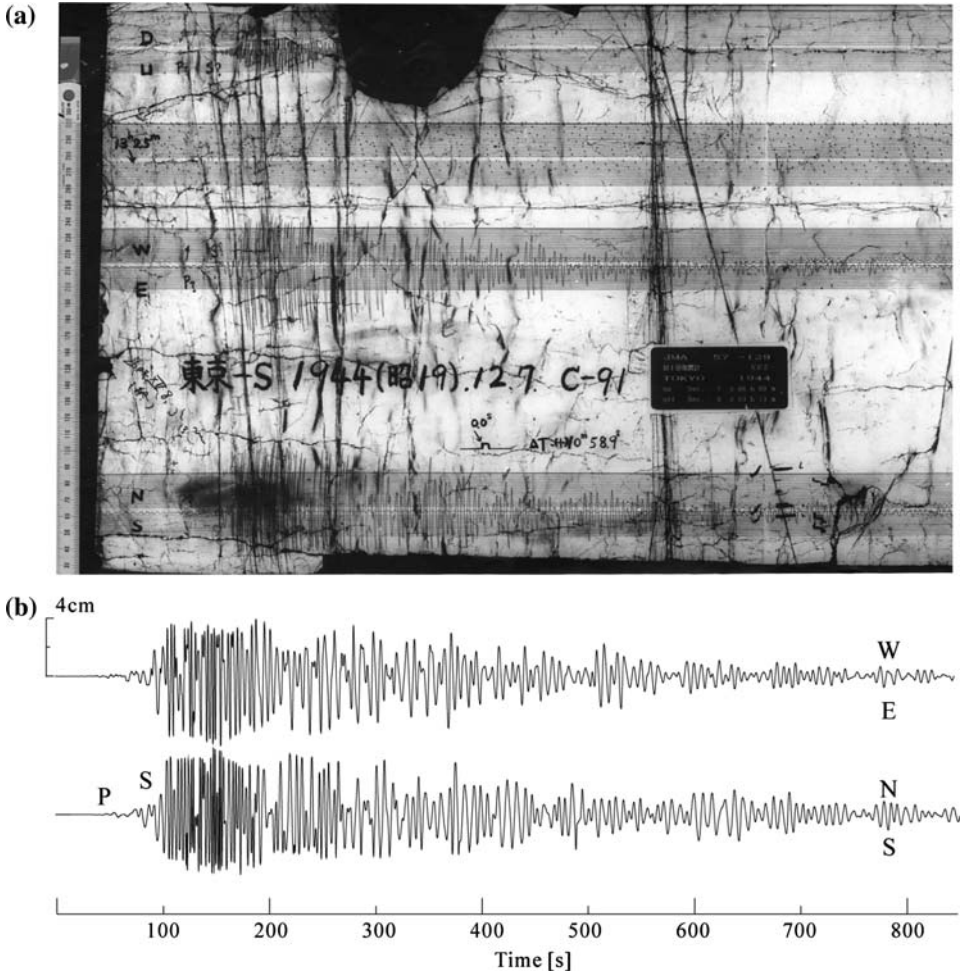


Figure 6

(a) Example of a smoked-paper seismogram from a CMO-type strong-motion instrument installed at Tokyo during the 1944 Tonankai Earthquake. (b) Digitized wave form data of the WE and NS components of displacement motions. Instrumental corrections were not applied to the seismograms.

Peninsula (Mw 7.4) earthquake in 2004, demonstrate a very large (>10 cm/s) and prolonged (>10 min) long-period ground-shaking at a dominant period of about 10–12 s.

#### 4. Computer Simulation of Long-period Ground Motions Arising from Earthquakes in the Nankai Trough

To complement the observational data for the two earthquakes that occurred in the Nankai Trough, we conducted computer simulations of seismic wave propagation using a

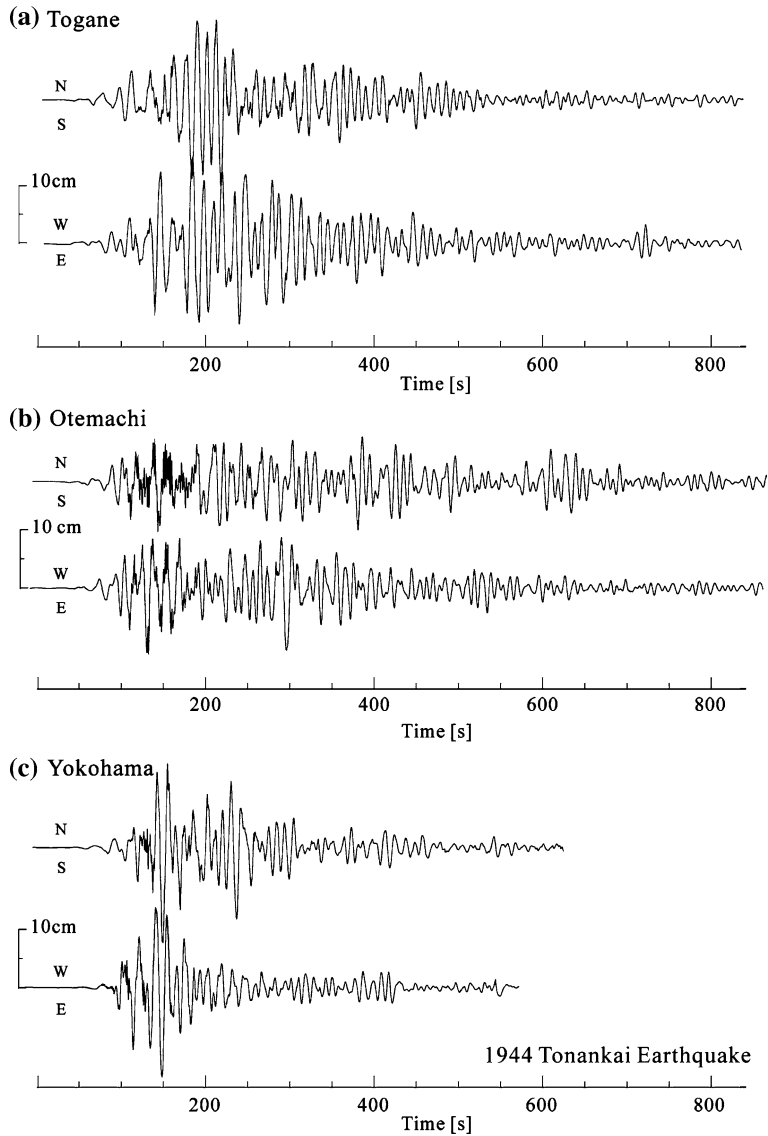


Figure 7

Wave forms of NS- and WE-component ground displacement motions during the 1944 Tonankai earthquake, as recorded at (a) Togan, (b) Otemachi, and (c) Yokohama. The instrumental responses of the strong-motion seismometers were corrected to reproduce the ground motions.

high-resolution structural model of central Japan and source-slip models for the earthquakes.

A structural model of the crust and upper-mantle beneath central Japan was recently developed from an analysis of reflection and refraction experimental data

(TANAKA *et al.*, 2006). A detailed structural model of the Nankai Trough subduction zone, with a shallowly dipping Philippine Sea Plate subducting beneath central Japan, has recently been investigated by compiling 29 profiles of reflection and refraction experiments (BABA *et al.*, 2006); this model was also included in the simulation model.

The simulation model covers an area of 496 km by 800 km, from the source region to Tokyo, and extends to a depth of 141 km. The model is discretized using a small mesh size of  $0.4 \times 0.4 \times 0.2$  km for depths less than 10 km and a large grid size of  $0.8 \times 0.8 \times 0.4$  km for areas from 10 to 141 km depth (Fig. 8).

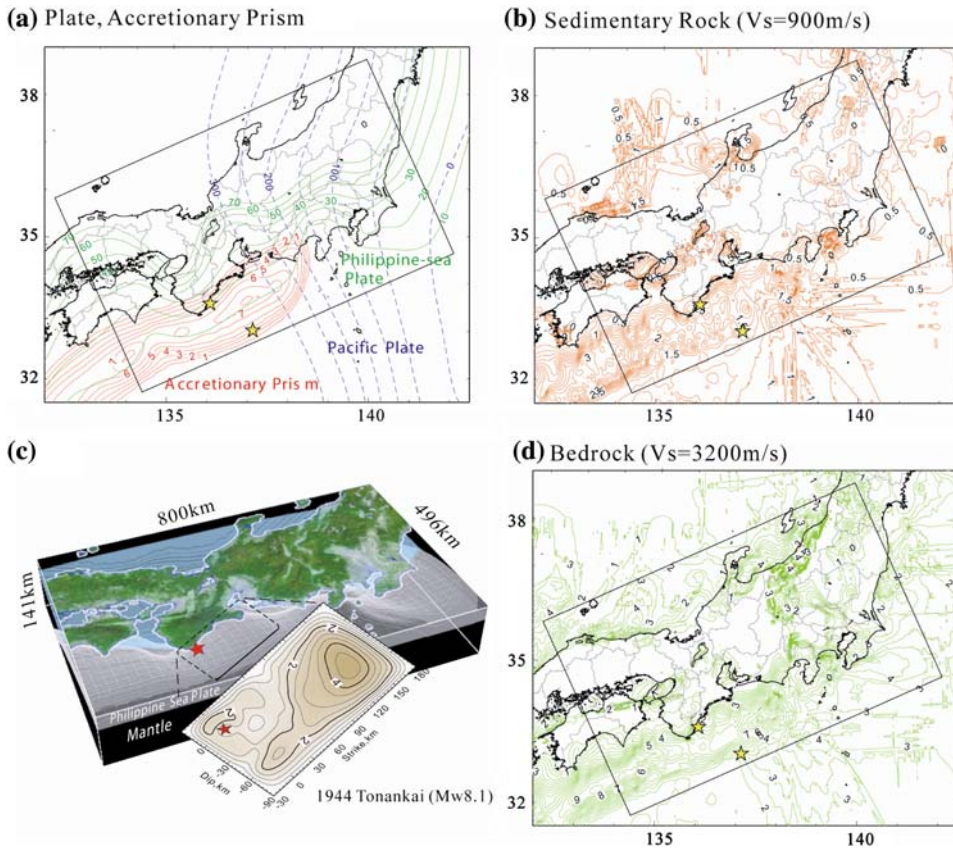


Figure 8

Structural model of central Japan used in the 3D wavefield calculations. (a) Outline of the study area, depth contours upon the subducting plates, and contours showing the thickness of the accretionary prism. (b) Depth distribution of the top of sedimentary layer with  $V_s = 900$  m/s. (c) Depth distribution of the top of bedrock with  $V_s = 3200$  m/s. (d) Details of the 3D model showing the configuration of the Philippine Sea Plate and the crust–mantle interface (Moho) and the source-slip model used for the 1944 Tonankai earthquake.

Table 1

*Physical parameters of P- and S-wave velocity, rock density, and anelastic attenuation coefficients for each layer represented in the simulation*

	Vp [km/s]	Vs [km/s]	$\rho$ [t/m <sup>3</sup> ]	Qp	Qs
Sedimentary Layer					
Layer 1	1.8	0.5	2.0	100	50
Layer 2	2.3	0.9	2.1	200	100
Layer 3	3.0	1.5	2.3	300	150
Basement	5.5	3.2	2.6	600	300
Upper Crust	5.8	3.3	2.7	700	350
Lower Crust	6.5	3.7	2.7	800	400
Upper Mantle	8.0	4.5	2.8	1000	500

The sedimentary structure of the Kanto Basin is constructed using three layers ( $V_s = 0.5, 0.9,$  and  $1.5$  km/s) overlying a rigid bedrock of  $V_s = 3.2$  km/s (TANAKA *et al.*, 2006). The physical parameters of P and S wavespeed ( $V_p, V_s$ ) and density ( $\rho$ ) and attenuation coefficients ( $Q_p, Q_s$ ) for the crust and upper-mantle structure and the subducting Philippine-Sea Plate are shown in Table 1. The Moho interface of the crust and upper-mantle boundary is based on the study of RYOKI (1999), and the depth of the mid-crustal (Conrad) interface is set to the middle of the crust.

The subducting Philippine Sea Plate consists of three layers of low-wavespeed oceanic layer 2 and layer 3 with a total thickness of 5 km, beneath which is a 25 km thickness of high-wavespeed oceanic mantle (BABA *et al.*, 2006). The cover of low-wavespeed sediments (accretionary prism) along the trench is also accommodated within the simulation model (Fig. 8a). The wavespeed in each layer of the subducting plate is assumed to increase linearly with depth ( $Z$ ) such that the physical parameters of the plate are assigned in the simulation model using the linear regression functions shown in Table 2.

The structural model employed in the simulation has been adjusted by matching predominant periods of observed ground motions at each station resulting from nearby earthquakes with theoretical estimates using physical parameters ( $V_p, V_s, \rho$  and thickness of each layer) of the structural model (TANAKA *et al.*, 2006). The comparison between observations and theoretical estimates indicates that the model is capable of simulating the nature of a long-period wavefield of roughly over 1–2 s.

Table 2

*Physical parameters of P- and S-wave velocity, rock density, and anelastic attenuation coefficients for each layer of the subducting plate and accretionary prism as a function of depth ( $Z$ ) from sea level*

	Vp [km/s]	Vs [km/s]	$\rho$ [t/m <sup>3</sup> ]	Qp	Qs
Accretionary Prism	3.5	1.5	1.8	90	50
Oceanic Layer 2	$5.4 + 0.0055*Z$	$V_p/1.94$	2.4	350	200
Oceanic Layer 3	$6.5 + 0.0055*Z$	$V_p/1.87$	2.5	500	300
Oceanic Mantle	$8.1 + 0.0053*Z$	$V_p/1.76$	2.8	850	500

The source-slip model for the 1944 Tonankai earthquake of YAMANAKA (2004a) has been estimated by an inversion using a near-field strong motion record and applying a low-pass filter with a cut-off frequency of 1 Hz. Thus the present simulation model of crust and upper-mantle structure in central Japan and source-slip model for the Tonankai earthquake is considered to be valid for simulating long-period ground motions of over about 1–2 s.

We did not include water column ( $V_p = 1.5$  km/s,  $V_s = 0$  km/s) in the present simulation model since such a low-wave speed layer below a free surface causes a serious instability problem during long-time FDM calculation due to a very large impedance contrast between water and low-wavespeed sedimentary layers at the coastal line area. Thus, our simulation underestimate the scattering and attenuation of P and S waves on the ocean side and it may underestimate the attenuation of P wave and elongation of P and S wave coda.

Seismic waves of relatively long-period ground motions over 1 s were calculated using a parallel, multi-grid Finite Difference Method (FDM; FURUMURA and CHEN, 2005), which uses a sixteenth -order staggered-grid FDM in horizontal ( $x$ ,  $y$ ) directions and a conventional fourth-order staggered-grid scheme in the vertical ( $z$ ) direction. The parallel FDM simulation is based on the domain-partitioning procedure: The 3D model is partitioned horizontally into a number of subregions assigned to numerous processors, and the message-passing interface (MPI) is used for inter-processor communications.

### 5. Computer Simulation of the 2004 Off-Kii Peninsula Earthquake

The source slip model used for the 2004 Off-Kii Peninsula earthquake was derived from an inversion using far-field wave-form data (YAMANAKA, 2004a). The size of the fault is  $60 \times 24$  km, with subfault segments of  $4 \times 4$  km. To implement the source slip model in the fine simulation grid, the source slip distribution was resampled into  $1 \times 1$  km subfaults using a linear interpolation function. A triangular source-slip function with a pulse width of 1 s was assigned to each subfault to radiate seismic waves with an assumed rupture propagation speed of  $V_r = 2.8$  km/s.

The results of the computer simulation of the SE Off-Kii Peninsula earthquake are shown in Figure. 9 as snapshots of horizontal ground velocity motions. It is interesting to compare the simulation results (Fig. 9a) with the observed wavefield recorded from the dense K-NET and KiK-net seismic array (Fig. 9b). Whereas the seismic observations are largely restricted to land areas and dense seismic observations are unavailable in oceanic areas, the computer simulation provides details of the propagation of seismic waves from the offshore source region to inland areas. The modeling results are therefore very useful in understanding the complex seismic behavior that occurs during propagation through the 3D heterogeneous structure of the subduction zone. Note that the simulated wavefield is slightly dominated by the relatively short-period band because the snapshots are produced from wave forms recorded at densely and equally (in 1.6 km) spaced



Figure 9

Comparison of snapshots of ground velocity associated with the 2004 SE Off-Kii Peninsula earthquake at uniform time interval ( $T = 60, 120, 180,$  and  $240$  s) from earthquake rupture, as derived from (a) observations from the dense strong-motion network (K-NET and KiK-net), and (b) computer simulation.

observation points (stations), while the observations are restricted to a relatively low density (20–25 km) of recording stations.

In the first snapshots shown in Figure 9 (60 s), large ground motions radiate from the source and approach coastal areas around the hypocenter. Ground-shaking has just begun in coastal areas, but the computer simulation demonstrates a dramatic oscillation of ground motions above the source region associated with the amplification of ground motions within the thick cover of low-wavespeed sediments (accretionary prism) in the Nankai Trough. The results of the simulation indicate that land-based observations of the

Nankai Trough earthquake capture only a portion of the complicated wavefield generated by the earthquake.

The middle snapshots in Figure 9 show the striking development of surface waves as they propagate along the Nankai Trough toward Tokyo. The directional guidance of long-period surface waves during interaction with low-wavespeed sediments is clearly evident. As the surface waves enter the Kanto Basin, the ground motion is further amplified within the thick cover basin sediments, resulting in long and strong wavetrains of long-period ground motions in central Tokyo ( $T = 240$  s).

This amplification and elongation of ground motions in the sedimentary basin is also clearly evident in other population centers, such as those in Osaka, Nagoya, and Toyama, in the  $T = 120$  and  $180$  s frames, but the greatest ground motion is recorded for Tokyo. The strong motions in Tokyo are caused by the directivity effect of the rupturing fault from southwest to northeast and thus the directional guidance of long-period seismic waves toward Tokyo along the Nankai Trough. Ground motion in other populated area such as those in Toyama and Osaka area appears to be underestimated in the simulation snapshots, indicating that we need further improvements in the structure in those areas by close comparison between observed and simulated ground motions using this and other large events. The relatively smooth wavefield of computer simulation as compared with the snapshots of the observed wavefield also indicate that the present model is rather smooth to recover the scattering effect of the short-period wavefield. It should also be noted here that the amplitude of the P wave derived by the simulation is very weak as compared with observations such as those illustrated in 120 s frame in Tokyo. This is probably due to the source-slip model used in the simulation which is mainly constructed by using the S wave form and thus it was not so match constrained by the waveform of P wave.

In Figure 10, simulated wave forms of NS-component ground velocity motions are compared with observed K-NET and KiK-net strong-motion records for seven stations aligned from the source region to Tokyo. A low-pass filter with a cut-off frequency of 1 Hz was applied to both simulated and observed seismograms. The simulated and observed seismograms show good agreement in terms of major features such as P- and S-wave arrival times, peak ground velocity, dominant period of the surface waves, and the envelope shape of later S-wave coda. This demonstrates the reliability of the structure model and source model employed in the simulation. However, the simulation results underestimate high-frequency waves beyond about 1-0.5 Hz, especially for near source stations such as MIEH04, AIC017 and SZOH37, indicating the limitation of the present simulation model for applying for strong motion simulations of relatively higher-frequency wavefields of over 1 Hz.

## 6. Computer Simulation of the 1944 Tonankai Earthquake

We then evaluated long-period ground motions arising from the 1944 Tonankai earthquake using a source-slip model of YAMANAKA (2004b). The size of the inferred fault



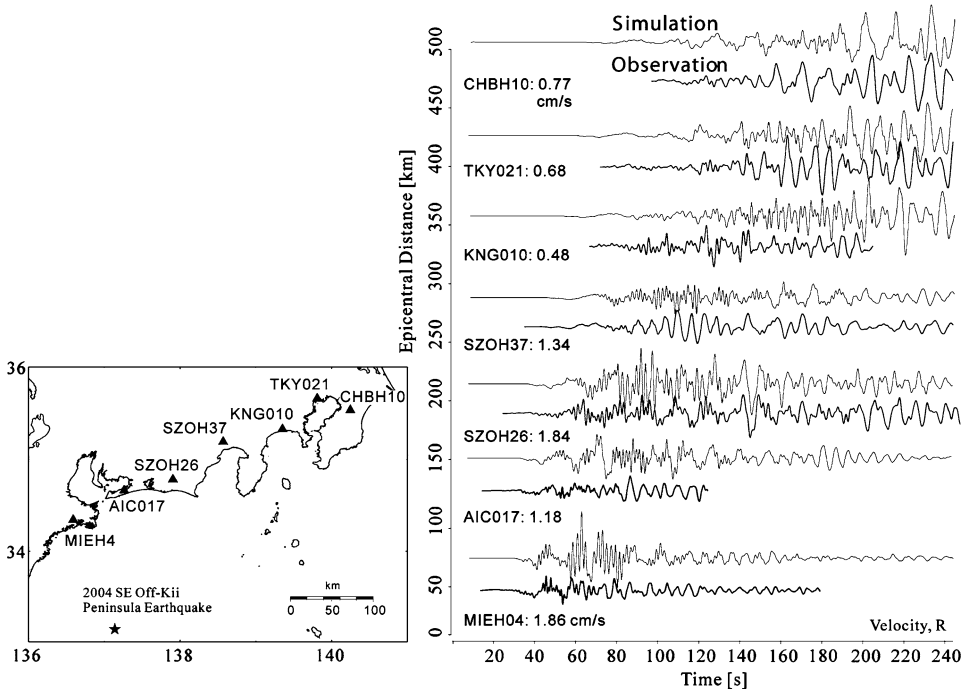


Figure 10

Comparison of simulated and observed wave forms of radial-component ground velocity motions at seven K-NET and KiK-net stations. Station locations are shown in the accompanying map.

is  $180 \times 90$  km, which was resampled into  $2 \times 2$  km subfaults using a linear interpolation function. A triangular slip-velocity function with a pulse width of 2 s was assigned to each subfault. As the inferred interpolated source-slip model might be producing a strong rupture-directivity effect along the direction of fault-rupture propagation, we introduced a random fluctuation in the fault-rupture speed at each point on the subfault. This random fluctuation is represented by a Gaussian function with a standard deviation of 5%, and the random fluctuation of rupture velocity is embedding over an average fault rupture speed of  $V_r = 2.95$  km/s.

Snapshots of simulated horizontal ground velocity motions during the 1944 Tonankai earthquake are shown in Figure 11 at time intervals of 60 s. Each snapshot clearly demonstrates the spreading of S waves from the M 8 source and the development of long-period ground motions via interaction with sedimentary structures in the Nankai Trough. The effect of the low-wavespeed sedimentary wedge in terms of guiding long-period surface waves to the east is clearly evident in the middle frames ( $T = 120$  and  $180$  s).

The snapshots capture the significant amplification of ground motions within large sedimentary basins such as those beneath Osaka, Nagoya, and Tokyo. This amplification was also detected in the observed wavefield during the 2004 SE Off-Kii Peninsula earthquake (Fig. 1, Fig. 8a).

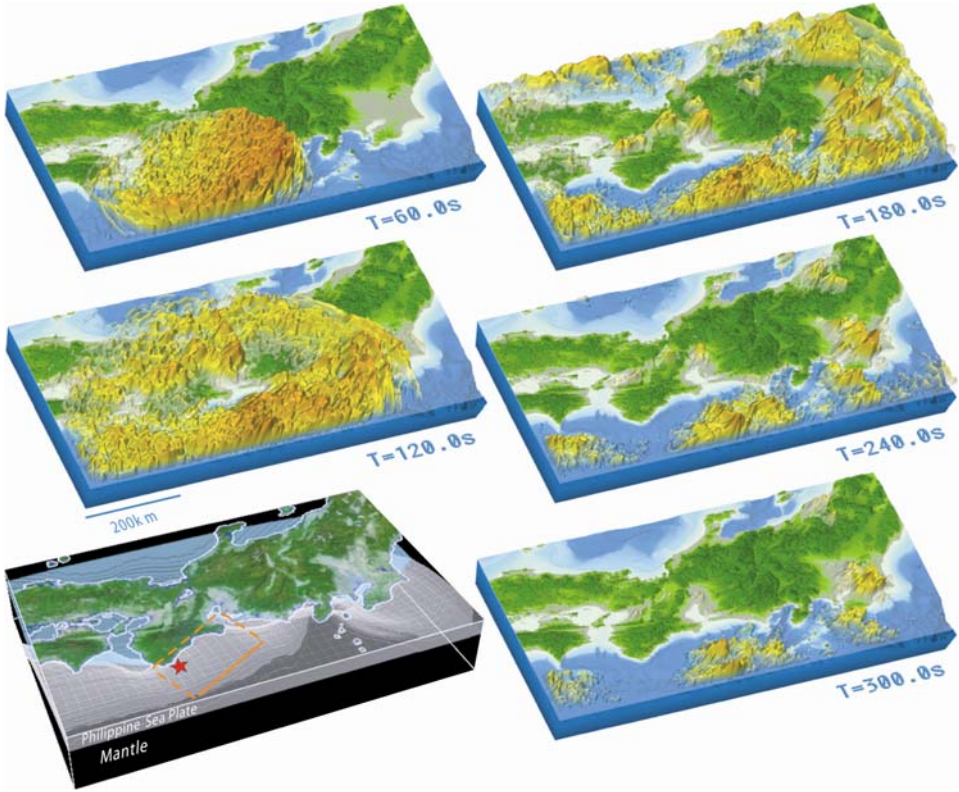


Figure 11

Snapshots of the propagation of simulated seismic waves arising from the 1944 Tonankai earthquake for  $T = 60, 120, 180, 240$  and  $300$  s from source rupture.

Central Tokyo is affected by prolonged ground-shaking for several minutes leading up to the propagation of the S-wave front across the Kanto Basin to the north ( $T = 300$  s). As the enhanced ground motions in the sedimentary basin are several times larger and longer than those observed during the 2004 SE Off-Kii Peninsula earthquake, so it might be a strong impact on modern large-scale constructions.

Figure 12 shows a comparison of the simulated waveforms of NS-component ground velocity motions and the velocity response spectra assuming  $h = 0.05$  damping constant with observational data recorded at Togane, Otemachi, and Yokohama during the Tonankai earthquake. A low-pass filter with a band pass frequency of 0.02–0.5 Hz was applied to the simulated and observed seismograms. The simulation results demonstrate the major features of observed ground motions such as the dominant period of the surface waves and the shape of the S wave and its coda. The levels of the velocity response spectra of observed and simulated ground motions are in good agreement, but some differences in the dominant period of peak ground motion are recorded for Togane and

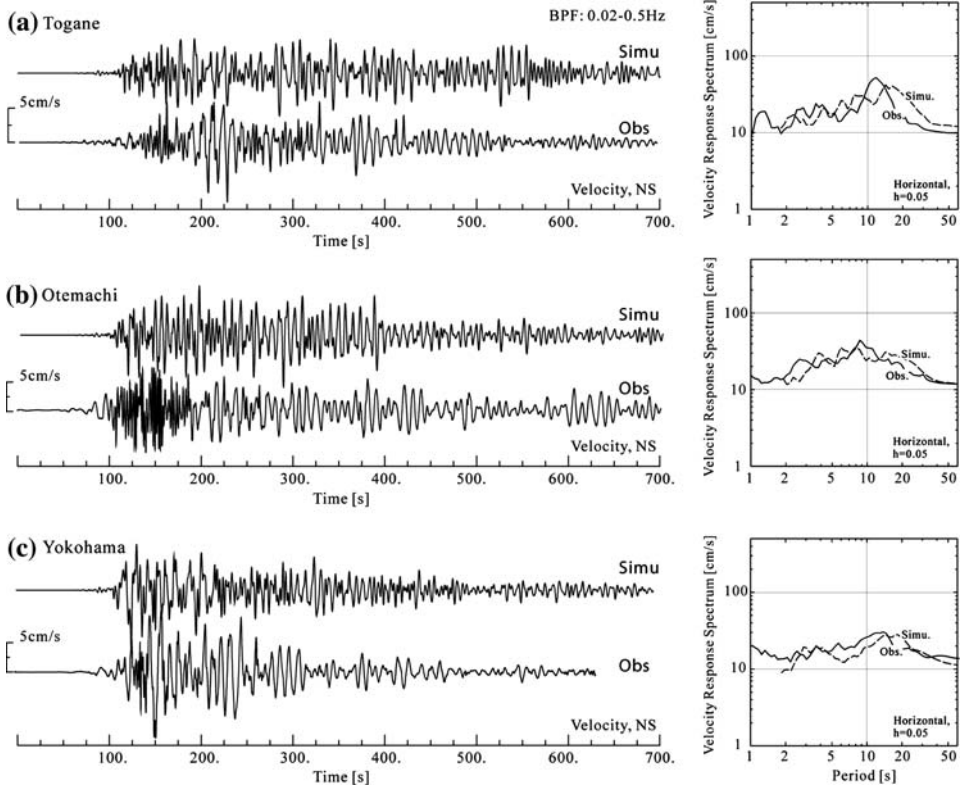


Figure 12

Comparison between the simulation (top) and observational data (bottom) in terms of the wave form of NS-component ground velocity motions and velocity response spectra recorded at (a) Togane, (b) Otemachi, and (c) Yokohama for the 1944 Tonankai earthquake.

Yokohama, probably due to limitations in the source model and uncertainties in the sedimentary structure model below these stations. However, the major features of the long-period ground motions developed within the Kanto Basin are well simulated by the present simulation, consequently we believe that the present model has largely attained the level of accuracy required to estimate the strength of long-period ground motions expected in central Tokyo during future earthquakes in the Nankai Trough.

The result of the computer simulation of the 1944 Tonankai earthquake also depicts strong ground motions within areas for which observational data were not available at the time due to a lack of seismic instruments or the fact that the seismometer was completely clipped due to intense ground-shaking (as occurred in near-fields such as in Osaka and Nagoya).

Figure 13 shows the simulated ground motions at stations located on major sedimentary basins, such as those at Osaka (OSK005), Nagoya (AIC003), Toyama

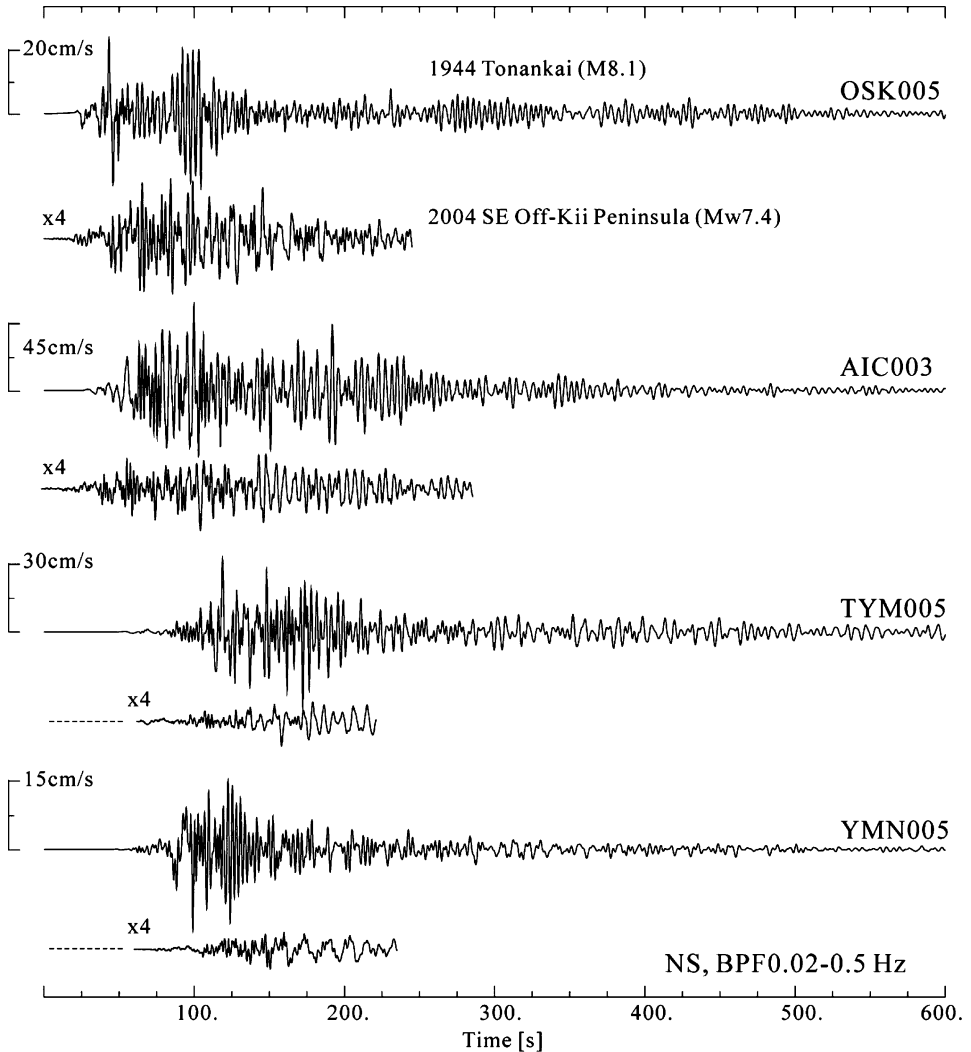


Figure 13

Simulated wave form of NS-component ground velocity motions for the 1944 Tonankai earthquake (top line) and comparison between observed wave forms from the 2004 SE Off-Kii Peninsula earthquake (bottom line, amplitude is multiplied by 4) at stations OSK005, AIC003, TYN005, and YMN005. A band pass filter of 0.02–0.5 Hz was applied to the wave forms.

(TYM005), and Kofu (YMN005). These results are compared with the observed ground motions for the 2004 SE Off-Kii Peninsula earthquake. It is apparent from the simulation that large and prolonged long-period ground motions occurred in major sedimentary basins following the occurrence of large earthquakes. The wave forms of the 1944 event are several times larger and longer than those of the 2004 earthquake. The dominant

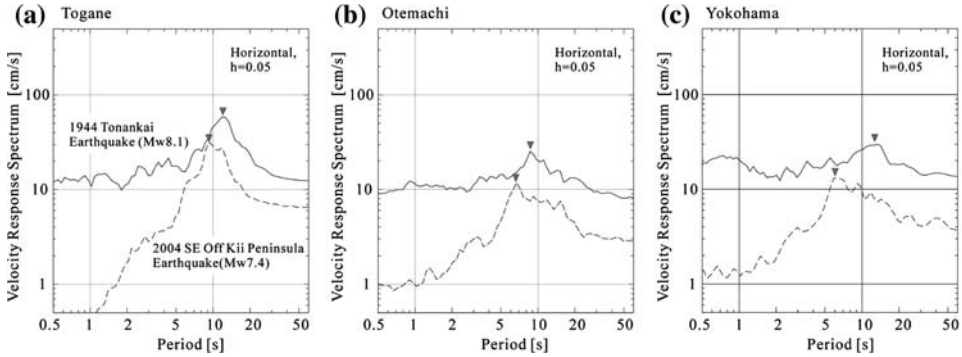


Figure 14

Comparison of the velocity response spectra for averaged horizontal motions from the 1944 Tonankai earthquake (solid lines) and the 2004 SE Off-Kii Peninsula earthquake, as recorded at stations OSK005, AIC003, TYM005, and YMN005.

period of long-period surface waves that developed in the basins is 2–3 s for Toyama and Kofu and 3–5 s for Osaka and Nagoya, approximately corresponding to the thicknesses of the basin sediments below the stations. The velocity response spectra for the 1944 Tonankai earthquake show a response that is approximately 10 times larger than that for the 2004 earthquake. This reflects the greater amplitude and longer duration of ground motions that arose from the Mw 8.1 earthquake.

## 7. Conclusions

The development of long-period ground motions with a predominant period of about 6–12 s by resonance in the thick cover of sedimentary layers beneath Tokyo is a common characteristic of all large events occurring around Tokyo, however the earthquakes in the Nankai Trough are expected to be the most disastrous in terms of producing extremely large and lengthy ground-shaking.

The strong motion record of the 1944 Tonankai Mw 8.1 earthquake demonstrates intense and prolonged shaking in central Tokyo associated with long-period ground motions with a dominant period of about 12–14 s. This finding highlights the potential vulnerability of modern large-scale construction to future earthquakes occurring in the Nankai Trough.

The present simulation model of crust and upper-mantle structure derived from the results of recent reflection and refraction experiments in central Japan and in the Kanto Basin and high-performance computing technology made possible the realistic simulation of long-period motions developing in the center of Tokyo during large earthquakes. However, the accuracy of the present model is rather limited in relatively longer-period bands over 1–2 s, and broadband simulation of strong ground motion including relatively

high-frequency signals over 1 Hz is still difficult due to uncertainties in the subsurface structure model and in the understanding of source-slip properties that affect the radiation and propagation of high-frequency seismic wavefields.

One of the important goals of strong-motion seismology is to predict the ground motions likely to occur in future earthquake scenarios and to assist in the development of appropriate building codes for different areas within sedimentary basins. Towards this goal, the improvements in the simulation model, especially the sedimentary structure beneath the Kanto Plain, are highly desired by maintaining a close link between computer simulations and observational studies that make use of the current high-density seismic network, archives of historical earthquakes.

### *Acknowledgements*

This study was supported by the Multi-Scale and Multi-Physics Integrated Simulation project (CREST) of the Japan Science and Technology Agency, and the Special Project for Earthquake Disaster Mitigation in Urban Areas funded by the Ministry of Education, Culture, Sports, and Science, Japan. The computer simulation was conducted using the Earth Simulator. The author acknowledges the Earth Simulator Center for their support with computer resources. K-NET and KiK-net data were provided by the National Institute for Earth Science and Disaster Research, Japan. Photographs of Imamura-type and CMO-type strong motion instruments shown in Figure 5 were provided from the Hamamatsu Collection of the Japan Meteorological Agency. The authors would like to thank Kim Olsen and one anonymous reviewer for thoughtful review comments and suggestions for revising the manuscript.

### REFERENCES

- BABA, T., ITO, A., KANEDA, Y., HAYAKAWA, T., and FURUMURA, T. (2006), *3D velocity structure model in the ocean around Japan inferred from controlled source seismic experiments*, Abst., Japan Geoscience Union Meeting, 2006.
- FURUMURA, T. and HAYAKAWA, T. (2007), *Anomalous propagation of long-period ground motions observed in Tokyo during the 23 October 2004 Niigata-ken Chuetsu (Mw 6.6) earthquake*, Bull. Seismol. Soc. Am. 97, 863–880.
- FURUMURA, T. and NAKAMURA, M. (2006), *Recovering of strong motion record of the 1944 Tonankai earthquake and long-period ground motion in Kanto region*, Geophys Exploration 59, 337–351, in Japanese.
- FURUMURA, T. and KENNETT, B.L.N. (2005), *Subduction zone guided waves and the heterogeneity structure of the subducting plate: Intensity anomalies in northern Japan*, J. Geophys. Res., 110, B10302, doi:10.1029/2004JB003484.
- FURUMURA, T., KENNETT, B.L.N., and KOKETSU, K. (2003), *Visualization of 3D wave propagation from the 2000 Tottori-ken Seibu, Japan, Earthquake: Observation and numerical simulation*, Bull. Seismol. Soc. Am. 93, 870–881.
- FURUMURA, T. and CHEN, L. (2005), *Parallel simulation of strong ground motions during recent and historical damaging earthquakes in Tokyo, Japan*, Parallel Computing, 31, 149–165.

- HATAYAMA, K., ZAMA, S., NISHI, H., YAMADA, M., and HIROKAWA, Y. (2004), *Long-period strong ground motion and damage to oil storage tanks due to the 2003 Tokachi-oki earthquake*, *Zisin* 57, 83–103.
- HATAYAMA, K., and ZAMA, S. (2005), *Sloshing of liquid in oil storage tanks and long-period strong ground motions due to 2004 M 7-class earthquakes southeast off the Kii Peninsula*, Report of National Research Institute of Fire and Disaster 99, 52–67.
- HAYAKAWA, T., FURUMURA, F., and YAMANAKA, Y. (2005), *Simulation of strong ground motions caused by the 2004 off the Kii Peninsula earthquakes*, *Earth Planets Space* 57, 191–196.
- KODAIRA, S., IIDAKA, T., NAKANISHI, A., PARK, J.-O., IWASAKI, T., and KANEDA, Y. (2005), *Onshore-offshore seismic transect from the eastern Nankai Trough to central Japan crossing a zone of the Tokai slow slip event*, *Earth Planets Space* 57, 943–959.
- KOKETSU, K., HATAYAMA, K., FURUMURA, T., IKEGAMI, Y., and AKIYAMA, S. (2005), *Damaging long-period ground motions from the 2003 Mw 8.3 Tokachi-oki, Japan, earthquake*, *Seismolol. Res. Lett.* 76, 1, 67–73.
- MIYAKE, H. and KOKETSU, K. (2005), *Long-period ground motions from a large offshore earthquake: The case of the 2004 off the Kii peninsula earthquake, Japan*, *Earth Planets Space* 57, 3, 203–207.
- NAKANISHI, A., TAKAHASHI, N., PARK, J.-O. PARK, MIURA, S., KODAIRA, S., KANEDA, Y., HIRATA, N., IWASAKI, T., and NAKAMURA, M. (2002), *Crustal structure across the coseismic rupture zone of the 1944 Tonankai earthquake, the central Nankai Trough seismogenic zone*, *J. Geophys. Res.* 107, doi:10.1029/2001JB000424.
- RYOKI, K. (1999), *Three-dimensional depth structure of the crust and upper-most mantle beneath southwestern Japan and its regional gravity anomalies*, *Zisin* 52, 51–63.
- SHAPIRO, N.M., OLSEN, K.B., and SINGH, S.K. (2000), *Wave-guide effects in subduction zones: Evidence from three-dimensional modeling*, *Geophys. Res. Lett.* 27, 433–436.
- TAKAHASHI, N., KODAIRA, S., NAKANISHI, A., PARK, J.-O., MIURA, S., TSURU, T., KANEDA, Y., SUEHIRO, K., and KINOSHITA, H. (2002), *Seismic structure of western end of the Nankai Trough seismogenic zone*, *J. Geophys. Res.* 107, doi:10.1029/2001JB000121.
- TANAKA, Y., MIYAKE, H., KOKETSU, K., FURUMURA, T., HAYAKAWA, T., BABA, T., SUZUKI, H., and MASUDA, T. (2006), *The DaiDaiToku integrated model of the velocity structure beneath the Tokyo metropolitan area (2)*, *Abst., Japan Geoscience Union Meet.* 2006, S116–P014.
- USAMI, T., *Materials of Comprehensive List of Destructive Earthquakes in Japan* (University of Tokyo Press, 1996).
- YAMANAKA, Y. (2004a), *Reanalysis of the 5 Sept. SE Off-Kii Peninsula earthquake (mainshock: Mj 7.4)*, EIC Seismological Note, Earthquake Research Institute, University of Tokyo, No.153.
- YAMANAKA, Y. (2004b), *Source process of the 1944 Tonankai and the 1945 Mikawa earthquake*, *Chikyu Monthly* 305, 739–745.

(Received September 6, 2006, revised January 1, 2007, accepted March 14, 2007)

Published Online First: April 2, 2008

---

To access this journal online:  
[www.birkhauser.ch/pageoph](http://www.birkhauser.ch/pageoph)

---